

Multi-Robot Informative Path Planning for Efficient Target Mapping using Deep Reinforcement Learning

Apoorva Vashisth¹, Dipam Patel¹, Damon Conover², Aniket Bera¹

¹Department of Computer Science, Purdue University, USA ²DEVCOM Army Research Laboratory, USA
{vashista, dipam, aniketbera}@purdue.edu, damon.m.conover.civ@army.mil

Abstract—Autonomous robots are being employed in several mapping and data collection tasks due to their efficiency and low labor costs. In these tasks, the robots are required to map targets-of-interest in an unknown environment while constrained to a given resource budget such as path length or mission time. This is a challenging problem as each robot has to not only detect and avoid collisions from static obstacles in the environment but also has to model other robots’ trajectories to avoid inter-robot collisions. We propose a novel deep reinforcement learning approach for multi-robot informative path planning to map targets-of-interest in an unknown 3D environment. A key aspect of our approach is an augmented graph that models other robots’ trajectories to enable planning for communication and inter-robot collision avoidance. We train our decentralized reinforcement learning policy via the centralized training and decentralized execution paradigm. Once trained, our policy is also scalable to varying number of robots and does not require re-training. Our approach outperforms other state-of-the-art multi-robot target mapping approaches by 33.75% in terms of the number of discovered targets-of-interest. We open-source our code and model at: https://github.com/AccGen99/mar1_ipp.

I. INTRODUCTION

Autonomous robotic systems are applicable in several tasks such as search-and-rescue missions [1, 2], environment mapping [3, 4], and orchard monitoring [5, 6]. Recently, multi-robot systems are gaining popularity for efficiently undertaking these tasks as opposed to single-robot systems [7], manual approaches [8], or conventional platforms. A key challenge in utilizing multi-robot systems is inter-robot collaboration in the presence of communication constraints, requiring careful planning for exchange of information.

In this work, we aim to utilize a multi-robot system to discover targets-of-interest in an unknown 3D environment while constrained to a resource budget, such as battery capacity. We consider presence of unknown obstacles in the environment and limited communication capability of the robots. Our multi-robot system consists of unmanned aerial vehicles (UAVs) equipped with a limited-range unidirectional sensor and a communication module with a limited transmission distance. We cast this problem as multi-robot informative path planning (MRIPP) problem, which aims to maximize the amount of information gathered by the multi-robot system operating under resource constraints. In our setting, trajectory planning is challenging due to unknown view-dependent occlusions in the 4D action space, i.e., the UAV 3D position and yaw angle, as well as consideration of

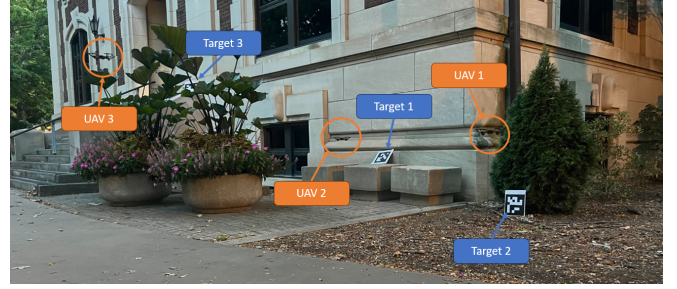


Fig. 1: Our reinforcement learning approach for MRIPP problem applied on Ryze Tello drones for real-world experiments with Aruco tags as targets-of-interest. By planning collision-free paths for the UAVs online, we maximize the number of targets discovered under flight-time constraints. We place 4 UAVs and 6 targets-of-interest in the environment, with 3 UAVs and 3 targets visible in the image.

trajectories planned by other robots not within the communication range. Applications for our approach include victim localization for disaster management (search and rescue), surveillance and reconnaissance in adversarial or complex environments for military applications, mapping fruits in an orchard, and discovering target-of-interest in urban scenarios.

Several approaches have been proposed for the MRIPP problem. Classical approaches [9–13] aim to extend the single-robot planners to multi-robot systems via sequential allocation where actions are planned for the robots one at a time in a specific sequence, instead of simultaneously. Later, centralized approaches [3, 14–22] were developed that involve one planner planning the next action for all robots simultaneously in their joint action space. Such planners consider infinite communication ranges within the environment and are not scalable with an increasing number of robots due to the explosion of the joint action space dimensions. Decentralized planners [23–30] aim to address these issues by allowing each robot to plan its own action, thus decoupling the action space. However, these methods do not directly apply to our problem setting since they do not consider limited communication range, 4D action space, inter-robot collisions, or unknown obstacles.

The main contribution of our work is a decentralized deep reinforcement learning solution for the MRIPP problem in an unknown 3D environment. We aim to maximize the discovered targets-of-interest while constrained to a resource budget. Our approach learns a single policy that can be implemented on any number of robots without significant performance degradation. The planner sequentially constructs

the trajectory for a robot within the multi-robot system based on the collected observations and remaining resource budget. A key aspect of our approach is an augmented graph representing the robot’s action space that aids in collision avoidance with both the static obstacles as well as other robots in the environment. Our augmented graph models the trajectories planned by all other robots using a gaussian process and restricts the planning to the robot’s local region. Fig. 1 illustrates our approach applied on unmanned aerial vehicles (UAV) in a realistic urban monitoring scenario.

In sum, we make the following three claims.

- Our approach scales to arbitrary number of robots without requiring retraining.
- Our method enables more efficient discovery of targets-of-interest, compared to state-of-the-art non-learning and learning-based methods in previously unseen environments.
- Our augmented graph encourages inter-robot communication and inter-robot collision avoidance by modeling trajectories of other robots in the multi-robot system.

We validate the performance of our approach in a urban monitoring application in a photorealistic simulator as well as conduct real robot experiments with multiple UAVs.

II. RELATED WORK

Multi-robot systems are extensively applied in exploration and mapping tasks. Classical approaches [9–13] attempt to extend the single-robot methods to multi-robot planning via sequential allocation [9] where one planner follows a specific order in sequentially planning the trajectories for each robot in the multi-robot system. Singh et al. [10] decompose the environment into clusters and plan a trajectory over the clusters, while Singh et al. [11] propose an adaptive receding-horizon approach. Hollinger and Singh [13] randomly generate the robot planning order and Luis et al. [12] utilize a deep reinforcement learning approach for ordering the planning sequence of the robots. However, these approaches consider only the effect of actions planned by robots earlier in the sequence and do not account for the potential cooperation within the multi-robot system that could be achieved via simultaneously planning next action for each robot.

Centralized planning approaches [3, 14–22] introduce cooperative behavior by planning in the joint action-space of all robots in the multi-robot system. Yilmaz et al. [14], Dutta et al. [15], Wei and Zheng [16] aim to minimize uncertainty associated with the given uncertainty map. Yoon and Qiao [3], Di Caro and Yousaf [17], Diop et al. [18], Cao et al. [21] decompose the environment into clusters and allocate one robot per region to divide-and-conquer the mapping task. La et al. [20] utilize a consensus filter for planning, while Barrionuevo et al. [19] rely on training a planner using deep reinforcement learning. Cui et al. [22] attempts to resolve potential collisions among given pre-computed trajectories. However, these planners require infinite communication range to communicate the collected observations and the next planned action for each robot. Moreover, these methods are not scale-able with increasing number of robots

as the joint action-space dimension explodes, leading to inapplicability of these approaches in real-time settings.

Decentralized planners [23–30] were introduced to provide scalable solutions to the MRIPP problem. These approaches allow each robot to individually plan their next action, decoupling the action space. Best et al. [27] propose a decentralized variant of Monte-Carlo tree search (MCTS) while Cui et al. [29], Julian et al. [30] utilize consensus filters for encouraging cooperation among the multi-robot system. Recently, deep reinforcement learning has been employed to learn robot policies for decentralized planning. These learned policies then sequentially construct the robot trajectory based on obtained observations. Deep reinforcement learning-based approaches are not only computationally efficient at deployment but also have the ability to generalize to similar environments not seen during training. Viseras and Garcia [23] utilize parameter sharing to encourage cooperation among robots. Westheider et al. [24], Venturini et al. [28] utilize the centralized training and decentralized execution paradigm while Yanes Luis et al. [26] employ Q-Learning to learn collision avoidance behaviour. Yang et al. [25] attempt to utilize attention mechanism for modeling the trajectories of other robots, termed intent, and encourage cooperative behaviour while utilizing a global representation. However, these approaches do not consider inter-robot collision avoidance [25, 26] or presence of unknown obstacles in the environment [28, 30]. A key difference with prior works is that our approach models the complete trajectory history of other robots, and our novel augmented graph restricts robot’s actions to its local area, enabling avoiding collisions with newly detected obstacles as well as preventing inter-robot collision. We show that our approach outperforms the state-of-the-art in both learning-based and non-learning baselines.

III. OUR APPROACH

We propose a novel deep reinforcement learning approach for MRIPP in unknown 3D environments. Fig. 2 overviews our approach for any robot in the multi-robot system. A major contribution of our approach is a graph representation we term as *augmented graph*. Our augmented graph models the probabilistic distribution of every other robots’ position and restricts planning to each robot’s known local region for collision avoidance with static obstacles. For each robot i , we estimate the utility value for each of its candidate actions in the current augmented graph as the number of targets observed upon executing it and its corresponding uncertainty using a Gaussian process [31]. We utilize another Gaussian process to model the probabilistic distribution of other robots’ locations and regress the mean and variance values for each candidate action. At each time-step, our policy network outputs a probability distribution over the candidate actions in the augmented graph. We use the obtained observations to train the utility and trajectory Gaussian processes, update the occupancy map, and generate rewards reflecting the MRIPP objective. An experience buffer collects the robot’s augmented graph, sampled action, predicted state

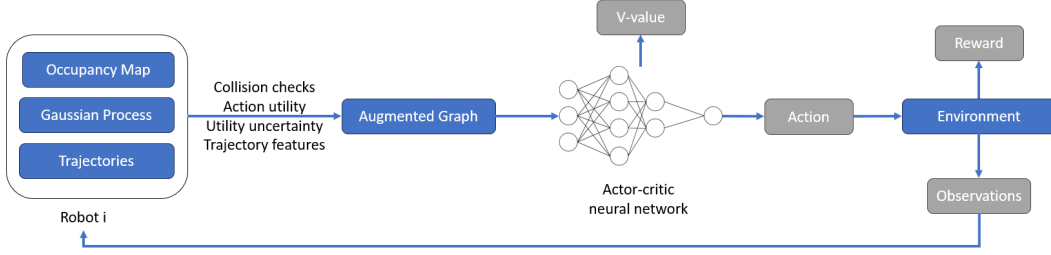


Fig. 2: Overview of our deep reinforcement learning based approach for MRIPP problem.

value, and reward over several training episodes to train the actor-critic network using on-policy reinforcement learning.

A. Environment

We aim to utilize a multi-robot system to map the distribution of targets-of-interest in an unknown 3D environment containing obstacles. We utilize Gaussian processes to model the view-dependent number of observed targets and the positions of other robots in the multi-robot system. Each robot maintains an occupancy map that aids in avoiding collisions with the detected static obstacles. Our multi-robot system consists of N robots and is given a total maximum budget $B \in \mathbb{R}^+$ defined as the sum of maximum cost of trajectory traversed by each robot. Hence, each robot $i \in [1, N]$ receives a budget of $B_i = B/N$. We model the workspace for each robot i , defined as \mathcal{A}_i , as a set of actions $\mathbf{a}_{i,j,t} = [x_{i,j,t}, y_{i,j,t}, z_{i,j,t}, d_{i,j,t}]^\top$ where $x_{i,j,t}, y_{i,j,t}, z_{i,j,t} \in \mathbb{R}$ are the 3D position coordinates within environment bounds and $d_{i,j,t} \in \mathcal{D}$ is the yaw of the unidirectional onboard sensor, e.g., an RGB-D camera. Our robots collect observations at each visited waypoint. The set \mathcal{D} denotes a user-defined set of possible robot yaw directions. At each mission time-step t and for each robot i , our approach plans over a set of L candidate actions in the set $\mathcal{A}_{i,t} \subseteq \mathcal{A}$ where $|\mathcal{A}_{i,t}| = L$. Each robot's candidate actions are sampled uniformly at random from its C -neighborhood around $\mathbf{a}_{i,t-1}$ within known free space, where C is a constant specifying the extent of the robot's local region. The reachability checks are performed for each candidate action along straight lines for collision avoidance with both the detected static obstacles and with other robots in the environment.

After executing an action $\mathbf{a}_{i,t}$, the robot i observes a certain number of targets. Each candidate action $\mathbf{a}_{i,j,t} \in \mathcal{A}$ is associated with its utility value $u(\mathbf{a}_{i,j,t}) \in \mathbb{R}^+$ reflecting the number of targets observed. The number of observed targets is normalized by a constant factor for stable policy training. As the utility function $u : \mathcal{A} \rightarrow \mathbb{R}^+$ is partially unknown for candidate actions $\mathbf{a}_{i,j,t}$, we utilize a Gaussian process for their estimation. Gaussian processes are widely used to estimate spatially correlated phenomena [31, 32]. We train a Gaussian process on the utility values of the previously executed actions and utilize the regressed utility values and the variance quantizing the uncertainty in the estimated utility values to inform the planning policy.

A Gaussian process is characterised by a mean function $m(\mathbf{a}_i) \triangleq \mathbb{E}[u(\mathbf{a}_i)]$ and a covariance function

$k(\mathbf{a}_i, \mathbf{a}'_i) \triangleq \mathbb{E}[(u(\mathbf{a}_i) - m(\mathbf{a}_i))(u(\mathbf{a}'_i) - m(\mathbf{a}'_i))]$ as $u(\mathbf{a}_i) \sim GP(m(\mathbf{a}_i), k(\mathbf{a}_i, \mathbf{a}'_i))$, where $\mathbb{E}[\cdot]$ is the expectation operator and $\mathbf{a}_i, \mathbf{a}'_i \in \mathcal{A}$. Hence, considering a set of candidate actions \mathcal{A}_t at time-step t for which we wish to infer the utility, let the actions in set \mathcal{A}_t correspond to a feature matrix \mathbf{A}_t , where each i^{th} row corresponds to the action vector $\mathbf{a}_i^t \in \mathcal{A}_t$. The set of all previously executed actions $\{\mathbf{a}_0, \mathbf{a}_2, \dots, \mathbf{a}_{t-1}\}$ is represented by feature matrix \mathbf{A}'_{t-1} . Utility values corresponding to previously executed actions are represented by the vector $\mathbf{u}'_{t-1} = [u(\mathbf{a}_1), \dots, u(\mathbf{a}_{t-1})]^\top$. We predict the utility values of candidate action set \mathcal{A}_t by conditioning the Gaussian process on the observed utility values $\mathbf{u}_t | \mathbf{A}'_{t-1}, \mathbf{u}'_{t-1}, \mathbf{A}_t \sim \mathcal{N}(\boldsymbol{\mu}, \mathbf{P})$:

$$\boldsymbol{\mu}(\mathbf{A}_t, \mathbf{A}'_{t-1}) = \mathbf{m}(\mathbf{A}_t) + \mathbf{K}(\mathbf{A}_t, \mathbf{A}'_{t-1}) [\mathbf{K}(\mathbf{A}'_{t-1}, \mathbf{A}'_{t-1}) + \sigma_n^2 \mathbf{I}]^{-1} (\mathbf{u}'_{t-1} - \mathbf{m}(\mathbf{A}'_{t-1})), \quad (1)$$

$$\mathbf{P}(\mathbf{A}_t, \mathbf{A}'_{t-1}) = \mathbf{K}(\mathbf{A}_t, \mathbf{A}_t) - \mathbf{K}(\mathbf{A}_t, \mathbf{A}'_{t-1}) [\mathbf{K}(\mathbf{A}'_{t-1}, \mathbf{A}'_{t-1}) + \sigma_n^2 \mathbf{I}]^{-1} \mathbf{K}(\mathbf{A}'_{t-1}, \mathbf{A}_t)^\top, \quad (2)$$

where $\sigma_n^2 \in \mathbb{R}^+$ is a hyperparameter describing the measurement noise variance, \mathbf{I} is an $n \times n$ identity matrix where $n = t - 1$, and $\mathbf{K}(\cdot, \cdot)$ corresponds to the covariance matrix.

B. Informative Path Planning

We model the path followed by a robot i in the multi-robot system as a sequence of consecutively executed actions $\psi_0^{i,T} = (\mathbf{a}_{i,0}, \mathbf{a}_{i,1}, \dots, \mathbf{a}_{i,T})$ where $\mathbf{a}_{i,0}$ denotes the start action, i.e. the initial robot pose, and $\mathbf{a}_{i,T}$ is the final action upon depletion of the budget $B_i = B/N$. The general MRIPP problem aims to find a set of optimal trajectories $\psi_0^{*,T} \in \Psi_{1:N}$ such that $\psi_0^{*,T} = [\psi_0^{1,T}, \psi_0^{2,T}, \dots, \psi_0^{N,T}]$ in the space of all possible paths $\Psi_{1:N}$ to optimize an information-theoretic objective function:

$$\psi_0^{*,T} = \operatorname{argmax}_{\psi_0^T \in \Psi_{1:N}} \sum_{i=1}^N I(\psi_0^{i,T}), \text{ s.t. } C(\psi_0^{i,T}) \leq B_i, \quad (3)$$

where $I : \Psi \rightarrow \mathbb{R}^+$ is the information gained from observations obtained by robot i upon executing a trajectory $\psi_0^{i,T}$ and the cost function $C : \Psi \rightarrow \mathbb{R}^+$ maps the trajectory $\psi_0^{i,T}$ to its execution cost.

Each robot i in our multi-robot system traverses a straight line between two consecutively executed actions. Observations are collected at each waypoint in the trajectory $\psi_0^{i,T}$ and are used to update the Gaussian processes, the occupancy map, and to generate a reward. Hence, we model the MRIPP

problem as a sequential decision-making process. Similar to Vashisth et al. [5], as we aim to maximize the number of observed targets, we define a function $\nu : \mathcal{A} \times \Psi \rightarrow \mathbb{R}^+$ as the number of new targets observed upon executing an action $\mathbf{a}_{i,t} \in \mathcal{A}$ by robot i after following the path $\psi_0^{i^{t-1}}$.

We define the information obtained along robot i 's trajectory as:

$$I(\psi_0^T) = \sum_{t=1}^T \nu(\mathbf{a}_{i,t}, \psi_0^{i^{t-1}}), \quad (4)$$

where we aim to plan ψ_0^T to maximise information I .

For informative planning, we leverage our two Gaussian processes defined in Section III-A to regress the utility and uncertainty associated with actions, as well as the mean and variance of the probability distribution of the positions of other robots in the multi-robot system. We utilize the reward structure as in previous works [5] considering the exploration-exploitation trade-off. At each time-step t , the robot i executes an action $\mathbf{a}_{i,t}$, collects observations, communicates with any nearby robots, and receives a reward $r_{i,t} \in \mathbb{R}^+$. The reward function consists of an exploration term $r_{e,t}$ and an information term $r_{u,t}$ such that $r_t = \alpha r_{e,t} + \beta r_{u,t}$ with:

$$r_{e,t} = \frac{\text{Tr}(\mathbf{P}(\hat{\mathbf{A}}_t, \mathbf{A}'_{t-1})) - \text{Tr}(\mathbf{P}(\hat{\mathbf{A}}_t, \mathbf{A}'_t))}{\text{Tr}(\mathbf{P}(\hat{\mathbf{A}}_t, \mathbf{A}'_{t-1}))}, \quad (5)$$

$$r_{u,t} = \nu(\mathbf{a}_{i,t}, \psi_0^{i^{t-1}}),$$

where $\text{Tr}(\cdot)$ is the trace operator of a matrix and α and β are constants used to trade off exploration and exploitation. Here, \mathbf{P}_u indicates the covariance matrix of the Gaussian process associated with utility regression. The variance reduction of the Gaussian process measures exploration $r_{e,t}$. Scaling the reward by $\text{Tr}(\mathbf{P}(\hat{\mathbf{A}}_t, \mathbf{A}'_{t-1}))$ stabilises the actor-critic network training [5, 32]. The term $r_{u,t}$ measures the new information gained after executing $\mathbf{a}_{i,t}$.

C. Augmented Graph

MRIPP requires each robot in the multi-robot system to reason about both the information distribution in the environment and the trajectories planned by other robots. Inspired by the dynamic graph approach for single-robot planning [5], we propose an augmented graph that models each robot's collision-free reachable action space, information distribution in the robot's neighborhood, and the probabilistic distribution of other robot's positions by sampling actions as defined in Section III-A. Our learned policy relies on the representation of the current knowledge about the environment in the augmented graph to predict next action Section III-D.

As the positions of the robots in the multi-robot system are unknown during certain time-steps due to communication constraints, we utilize another Gaussian process to model the probabilistic distribution of the robots' positions. At each time-step, t , our robot i within our multi-robot system executes an action $\mathbf{a}_{i,t}$ and arrives within the communication range of some, but not all, other robots. We consider a

single-hop communication paradigm and assume the maximum range of communication as $R \in \mathbb{R}^+$. We consider robot i to be communicating with robot k at time-step t if the euclidean distance p between the robots is less than maximum range $p(\mathbf{a}_{i,t-1}, \mathbf{a}_{k,t-1}) < R$. The communicating robots share their occupancy maps, candidate actions at time-step t , and their executed trajectories. Each robot i maintains its own Gaussian process to model the position distribution of the other robots it has communicated with. As the robots communicate, the Gaussian process for each robot is updated with the newly acquired waypoints. To further account for the future positions of other robots, we associate each action $\mathbf{a}_{i,t} \in \mathcal{A}$ in the workspace of robot i with the mean and variance values regressed from this Gaussian process.

At each time-step t , we re-build a fully connected graph $\mathcal{G}_{i,t} = (\mathcal{N}_{i,t}, \mathcal{E}_{i,t})$ for each robot i in the multi-robot system, where the node set $\mathcal{N}_{i,t}$ is the set of candidate actions $\mathcal{A}_{i,t}$ defined in Section III-A, to account for newly gathered observations. In this work, we consider a multi-robot system of holonomic UAVs defined as the sum of the actions' Euclidean distance and a small constant cost C_s if robot i 's yaw d_i changes.

To better inform the planning policy, we leverage our Gaussian processes to create node features utilized in our actor-critic network. At each time-step t , the node feature matrix $\mathbf{M}_{i,t}$ of robot i 's graph $\mathcal{G}_{i,t}$ consists of its candidate actions, the utility and uncertainty values queried from the Gaussian process modeling the environment, and the mean and variance values queried from the Gaussian process modeling the trajectories. The n^{th} row of $\mathbf{M}_{i,t}$ relates to the n^{th} action of robot i :

$$\mathbf{M}_{i,t}(i) = [\mathbf{a}_{i,n,t}, m_u(\mathbf{a}_{i,n,t}), k_u(\mathbf{a}_{i,n,t}, \mathbf{a}_{i,n,t}), m_t(\mathbf{a}_{i,n,t}), k_t(\mathbf{a}_{i,n,t}, \mathbf{a}_{i,n,t})], \quad (6)$$

where $\mathbf{a}_{i,n,t} = [x_{i,n,t}, y_{i,n,t}, z_{i,n,t}, d_{i,n,t}]^\top$, $m_u(\mathbf{a}_{i,n,t})$, $k_u(\mathbf{a}_{i,n,t}, \mathbf{a}_{i,n,t})$ are the regressed utility and uncertainty values for action $\mathbf{a}_{i,n,t}$, and $m_t(\mathbf{a}_{i,n,t})$ and $k_t(\mathbf{a}_{i,n,t}, \mathbf{a}_{i,n,t})$ are the regressed mean and variance for trajectory modeling of other robots.

D. Actor-Critic Neural Network for Reinforcement Learning

For each robot i we utilize the augmented graph to model the collision-free actions for the planning policy to reason about and represent the current knowledge of the information distribution in the environment. As the Gaussian processes only predict the utility of greedily executing a single next action, we use reinforcement learning to train our policy for informative path planning over long-horizon paths.

We use an attention-based neural network to parameterize our stochastic planning policy $\pi(\mathcal{G}_{i,t}, \psi_0^{i^{t-1}}, B_{i,r}) \in [0, 1]^L$ that predicts a probability distribution over all L actions $\mathcal{A}_{i,t}$ based on the current dynamic graph $\mathcal{G}_{i,t}$, previously executed path $\psi_0^{i^{t-1}}$, and the remaining budget $B_{i,r}$. We follow the network structure proposed by Cao et al. [32] consisting of an encoder and a decoder module. The attention-based encoder learns the dependencies between actions in $\mathcal{G}_{i,t}$.

We condition the learned actions’ latent dependencies on a planning state consisting of previously executed actions ψ_0^{t-1} , and the remaining budget $B_{i,r}$. A budget mask filters out actions not reachable within the remaining budget. Based on the conditioned latent action dependencies, a decoder outputs a probabilistic policy reasoning over all actions in the dynamic graph. During training, the decoder also estimates the value function $V(\mathcal{G}_{i,t}, \psi_0^{t-1}, B_{i,r}) \in \mathbb{R}$ following the current policy $a_{i,t} \sim \pi(\mathcal{G}_{i,t}, \psi_0^{t-1}, B_{i,r})$. The estimated values, sampled actions, augmented graphs, planning states, and rewards collected by each robot throughout the training episode are stored in the experience buffer that is utilized to train the policy with an on-policy actor-critic reinforcement algorithm under centralized training and decentralized execution paradigm. In this work, we use proximal policy optimization [33]. During deployment, at each time step t , we choose the most informative action from $\pi(\mathcal{G}_{i,t}, \psi_0^{t-1}, B_{i,r})$.

IV. EXPERIMENTS

A. Setup

Environment. We test our approach in an urban monitoring scenario consisting of buildings and windows bounded in a scale-agnostic unit cube. Each robot in our multi-robot system maintains an occupancy map with $50 \times 50 \times 50$ voxels. In test environments, buildings are generated at random positions but are arranged in a regularly spaced 5×5 array during training. In both cases, windows are attached to generated buildings at random positions. The occupancy grid map of the environment is initialized as unknown space and is updated via sensor observations with free space, observed windows, and buildings. We tune the hyperparameters of our gaussian process in a small representative environment using the Matérn 1/2 kernel. For our reward function defined in Equation (3), we set $\alpha = 20.0$ and $\delta = 0.02$ to keep values of both terms numerically similar.

We consider each robot as a UAV platform with an onboard RGB-D camera of 90° field of view (FoV). Since the confidence in discovered targets decreases with distance, we constrain the maximum detection range to 30% of the environment size. The UAVs can communicate with a maximum transmission distance $R = 0.3$. The UAV can choose between yaw angles of $\{0, \frac{\pi}{2}, \pi, \frac{3\pi}{2}\}$ rad at the current altitude. Note that our method can be easily extended to finer discretizations.

Training. An episode consists of a multi-UAV system in a mission with budget B . We train in a structured environment as a randomly initialized policy learns efficiently from this structure and transfers to randomized test environments. The total number of windows varies between 200 and 250. We fix the number of waypoints in the augmented graph of each robot to 20 and set the initial pose of each UAV to $[0, 0, 0, \frac{\pi}{2}]^\top$. To keep our policy scale-agnostic, we normalize the robot’s internal environment representation and action coordinates. Hence, the budget B is unitless and randomly generated for each episode within the range $[7, 9]$.

We terminate an episode if the maximum number of executed actions exceeds 256. We run 36 environment instances

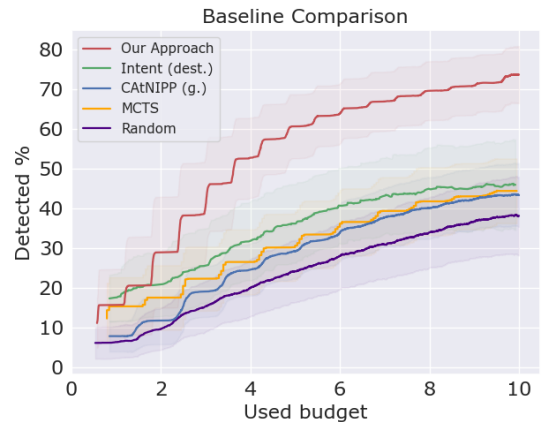


Fig. 3: Comparison of our approach against baselines in a UAV-based urban environment. Solid lines indicate means over 250 trials and shaded regions show standard deviations. Our approach outperforms other state-of-the-art learning-based and non-learning approaches by more efficiently discovering targets during a mission.

TABLE I: Comparison of our approach against baselines in a UAV-based target mapping scenario.

Baseline	% targets	Time (s)
Our approach	73.53 ± 6.83	1.74
Intent (dest.)	48.71 ± 7.60	25.39
CATNIPP (g.)	44.74 ± 7.96	30.83
MCTS	47.03 ± 7.60	292.69
Random agent	40.08 ± 9.65	0.06

in parallel to speed up episode generation. The policy is trained for 8 epochs using a batch size of 1024 and the Adam optimizer with a learning rate of 10^{-4} , which decays by a factor of 0.96 each 512 optimization steps. The policy gradient epsilon-clip parameter is set to 0.2. Our model is trained on a cluster equipped with Intel(R) Xeon(R) CPUs @ 3.60GHz and one NVIDIA A30 Tensor Core GPU. Our policy is trained for $\sim 120,000$ environment interactions.

B. Baseline Comparison

We show that our approach outperforms state-of-the-art baselines. We generate 25 test environments with different random seeds and run 10 trials on each environment instance with a budget of 10 units. We compare against: (i) Intent with destination modeling with a zero-shot policy (Intent dest.) where the highest probability action is executed; (ii) CATNIPP [32] extended by sequential allocation [9] with a zero-shot policy (CATNIPP g.); (iii) non-learning Monte Carlo Tree Search [34] (MCTS); (iv) a random policy on $L = 80$ augmented graph construction (random agent). To evaluate planning performance, we measure the percentage of discovered targets-of-interest during the test. We also report average replanning time.

We choose the destination intent variant [25] as our learning-based baseline, the state-of-the-art approach closest to our work, which uses global graph-based planning and infinite communication range. Since they do not consider collisions in the environment and modifying their approach to account for collisions is a non-trivial task, we allow the UAV to pass through obstacles to ensure a fair comparison.

TABLE II: Trajectory modeling ablation study.

Approach	% targets
With trajectory modeling	73.53 ± 6.83
Without trajectory modeling	69.46 ± 6.65

TABLE III: Scalability of our approach with number of robots N in the multi-robot system. The columns and rows indicate value of N in training and test environment, respectively.

	$N = 2$	$N = 3$	$N = 4$
$N = 2$	68.37 ± 6.95	66.84 ± 7.12	65.35 ± 7.49
$N = 3$	74.08 ± 6.52	73.53 ± 6.83	73.96 ± 6.79
$N = 4$	78.38 ± 5.62	76.76 ± 6.82	77.45 ± 7.96

Fig. 3 and Table I demonstrate our results. Our approach outperforms all baselines by a significant margin. In Table I, the approaches using reinforcement learning require significantly less planning time than non-learning methods, justifying the use of learning-based strategies.

C. Ablation Studies

Trajectory Modeling. We compare our approach trained with and without trajectory modeling. We compare the % discovered targets-of-interest for both approaches. Table II summarises the results. As the performance improves upon inclusion of trajectory modeling during training stage, we conclude that our augmented graph can actively reason about the positions of other robots for trajectory planning in our problem setting.

Scaling with N . We compare our approach trained with $N = \{2, 3, 4\}$ with different values of N in test environments. Table III illustrates the results. We observe similar performance of our transferred policies as compared to the trained policies. This can be attributed to the nature of our augmented graph, which does not require prior knowledge of the number of robots in the environment.

D. Simulation

We demonstrate the applicability of our deep reinforcement learning approach for MRIPP in an urban monitoring scenario created with Unreal Engine and AirSim. The Airsim simulator resembles real-world UAV dynamics, while Unreal Engine provides photorealistic imagery. Our urban environment is bounded by a $95\text{ m} \times 95\text{ m} \times 18\text{ m}$ cuboid. We utilize the Houses3K dataset [35] as illustrated in Fig. 4. We assume perfect localization and use ground truth window discovery. The UAV moves at a maximum speed of 2 m/s .

We compare our approach trained in the synthetic simulation described in Section IV-A against a random planner over our $L = 80$ augmented graph to reflect performance lower bound. Our metric for evaluating performance is defined as the percentage of discovered windows, and we record the coordinates of discovered windows to prevent multiple-counting of the same target. Similar to previous works [5, 32], our results are reported in the simulator with a mission budget of 7.0 units. Table IV compares the two planners. Our approach outperforms non-informative random planning.

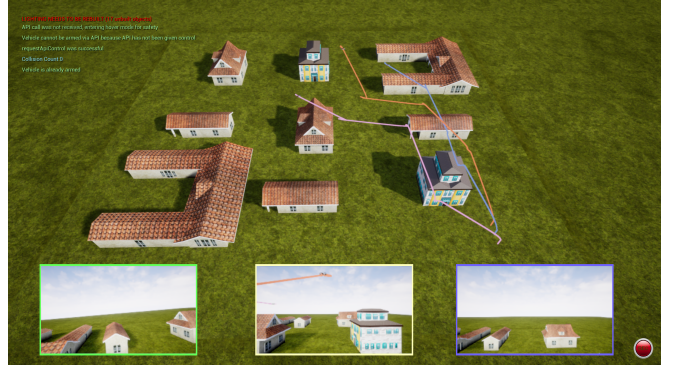


Fig. 4: Our approach implemented on a multi-robot system consisting of UAVs in photorealistic urban mapping scenario. We place 3 UAVs and 185 targets in the environment. We trace the path planned by each UAV with colored tracelines. The inset windows show the onboard camera view for each UAV.

TABLE IV: Comparison of our deep reinforcement learning-based approach against baselines in an urban monitoring simulator.

Approach	% targets
Our Approach	72.07 ± 11.04
Random Planner	50.39 ± 10.89

E. Implementation

We demonstrate the real-world applicability of our method by implementing on a multi-robot system for target mapping as illustrated in Fig. 1. We carried out experiments on 3 Ryze Tello drones in a $4.5 \times 4.5 \times 2.0\text{ m}^3$ arena containing randomly placed obstacles and targets. We place 6 Aruco tags and the UAVs are tasked with discovering the tags within a flight time of 15 minutes. The UAVs are equipped with a forward-facing camera to detect the tags.

V. CONCLUSION

We present a novel deep reinforcement learning approach for MRIPP problem in an unknown 3D environment. Our augmented graph-based approach models the trajectories of other robots in the multi-robot system for efficiently discovering targets of interest in an unknown 3D environment. Our experimental results support our three claims: (i) our approach is able to scale to any number of robots without requiring re-training; (ii) our approach outperforms the state-of-the-art learning-based approaches and non-learning baselines in environments unseen during training; (iii) our augmented graph enables modeling trajectories of other robots to prevent both inter-robot and robot-obstacle collisions. We validate our approach in a UAV-based urban mapping scenario as well as conduct real robot experiments to demonstrate the practical applicability. Future research directions include extending our approach for other multi-robot tasks such as pathfinding, task allocation, and collective robot construction.

ACKNOWLEDGMENT

This material is based upon work supported in part by the DEVCOM Army Research Laboratory under cooperative agreement W911NF2020221.

REFERENCES

- [1] J. Berger and N. Lo, "An innovative multi-agent search-and-rescue path planning approach," *Computers & Operations Research*, vol. 53, pp. 24–31, 2015.
- [2] J. R. Cooper, "Optimal multi-agent search and rescue using potential field theory," in *AIAA Scitech 2020 Forum*, 2020, p. 0879.
- [3] S. Yoon and C. Qiao, "Cooperative search and survey using autonomous underwater vehicles (auvs)," *IEEE Transactions on Parallel and Distributed Systems*, vol. 22, no. 3, pp. 364–379, 2010.
- [4] H. Bayerlein, M. Theile, M. Caccamo, and D. Gesbert, "Multi-uav path planning for wireless data harvesting with deep reinforcement learning," *IEEE Open Journal of the Communications Society*, vol. 2, pp. 1171–1187, 2021.
- [5] A. Vashisth, J. Ruckin, F. Magistri, C. Stachniss, and M. Popovic, "Deep reinforcement learning with dynamic graphs for adaptive informative path planning," *IEEE Robotics and Automation Letters*, 2024.
- [6] R. R. Shamshiri, C. Weltzien, I. A. Hameed, I. J. Yule, T. E. Grift, S. K. Balasundram, L. Pitonakova, D. Ahmad, and G. Chowdhary, "Research and development in agricultural robotics: A perspective of digital farming," *International Journal of Agricultural and Biological Engineering*, vol. 11, no. 4, pp. 1–14, 2018.
- [7] Y. U. Cao, A. B. Kahng, and A. S. Fukunaga, "Cooperative mobile robotics: Antecedents and directions," *Robot colonies*, pp. 7–27, 1997.
- [8] J. Su, X. Zhu, S. Li, and W.-H. Chen, "AI meets UAVs: A survey on AI empowered UAV perception systems for precision agriculture," *Neurocomputing*, vol. 518, pp. 242–270, 2022.
- [9] A. Singh, A. Krause, C. Guestrin, W. Kaiser, and M. Batalin, "Efficient planning of informative paths for multiple robots," in *Proceedings of the 20th international joint conference on Artificial intelligence*, 2007, pp. 2204–2211.
- [10] A. Singh, A. Krause, C. Guestrin, and W. J. Kaiser, "Efficient informative sensing using multiple robots," *Journal of Artificial Intelligence Research*, vol. 34, pp. 707–755, 2009.
- [11] A. Singh, A. Krause, and W. J. Kaiser, "Nonmyopic adaptive informative path planning for multiple robots," in *Proceedings of the 21st International Joint Conference on Artificial Intelligence*, 2009, pp. 1843–1850.
- [12] S. Y. Luis, D. Shutin, J. M. Gómez, D. G. Reina, and S. T. Marín, "Deep reinforcement multi-agent learning framework for information gathering with local gaussian processes for water monitoring," *arXiv preprint arXiv:2401.04631*, 2024.
- [13] G. Hollinger and S. Singh, "Multi-robot coordination with periodic connectivity," in *2010 IEEE International Conference on Robotics and Automation*. IEEE, 2010, pp. 4457–4462.
- [14] N. K. Yilmaz, C. Evangelinos, P. F. Lermusiaux, and N. M. Patrikalakis, "Path planning of autonomous underwater vehicles for adaptive sampling using mixed integer linear programming," *IEEE Journal of Oceanic Engineering*, vol. 33, no. 4, pp. 522–537, 2008.
- [15] A. Dutta, A. Ghosh, and O. P. Kreidl, "Multi-robot informative path planning with continuous connectivity constraints," in *2019 international conference on robotics and automation (ICRA)*. IEEE, 2019, pp. 3245–3251.
- [16] Y. Wei and R. Zheng, "Multi-robot path planning for mobile sensing through deep reinforcement learning," in *IEEE INFOCOM 2021-IEEE Conference on Computer Communications*. IEEE, 2021, pp. 1–10.
- [17] G. A. Di Caro and A. W. Z. Yousaf, "Multi-robot informative path planning using a leader-follower architecture," in *2021 IEEE International Conference on Robotics and Automation (ICRA)*. IEEE, 2021, pp. 10 045–10 051.
- [18] D. S. Diop, S. Y. Luis, M. P. Esteve, S. L. T. Marín, and D. G. Reina, "Decoupling patrolling tasks for water quality monitoring: A multi-agent deep reinforcement learning approach," *IEEE Access*, 2024.
- [19] A. M. Barrionuevo, S. Y. Luis, D. G. Reina, and S. L. T. Marín, "Informative deep reinforcement path planning for heterogeneous autonomous surface vehicles in large water resources," *IEEE Access*, 2024.
- [20] H. M. La, W. Sheng, and J. Chen, "Cooperative and active sensing in mobile sensor networks for scalar field mapping," *IEEE Transactions on Systems, Man, and Cybernetics: Systems*, vol. 45, no. 1, pp. 1–12, 2014.
- [21] N. Cao, K. H. Low, and J. M. Dolan, "Multi-robot informative path planning for active sensing of environmental phenomena: A tale of two algorithms," *arXiv preprint arXiv:1302.0723*, 2013.
- [22] R. Cui, B. Gao, and J. Guo, "Pareto-optimal coordination of multiple robots with safety guarantees," *Autonomous Robots*, vol. 32, pp. 189–205, 2012.
- [23] A. Viseras and R. Garcia, "Deepig: Multi-robot information gathering with deep reinforcement learning," *IEEE Robotics and Automation Letters*, vol. 4, no. 3, pp. 3059–3066, 2019.
- [24] J. Westheider, J. Rückin, and M. Popović, "Multi-uav adaptive path planning using deep reinforcement learning," in *2023 IEEE/RSJ International Conference on Intelligent Robots and Systems (IROS)*. IEEE, 2023, pp. 649–656.
- [25] T. Yang, Y. Cao, and G. Sartoretti, "Intent-based deep reinforcement learning for multi-agent informative path planning," in *2023 International Symposium on Multi-Robot and Multi-Agent Systems (MRS)*. IEEE, 2023, pp. 71–77.
- [26] S. Yanes Luis, M. Perales Esteve, D. Gutiérrez Reina, and S. T. Marín, "Deep reinforcement learning applied to multi-agent informative path planning in environmental missions," in *Mobile Robot: Motion Control and Path Planning*. Springer, 2023, pp. 31–61.
- [27] G. Best, O. M. Cliff, T. Patten, R. R. Mettu, and R. Fitch, "Decmcts: Decentralized planning for multi-robot active perception," *The International Journal of Robotics Research*, vol. 38, no. 2-3, pp. 316–337, 2019.
- [28] F. Venturini, F. Mason, F. Pase, F. Chiariotti, A. Testolin, A. Zanella, and M. Zorzi, "Distributed reinforcement learning for flexible uav swarm control with transfer learning capabilities," in *Proceedings of the 6th ACM workshop on micro aerial vehicle networks, systems, and applications*, 2020, pp. 1–6.
- [29] R. Cui, Y. Li, and W. Yan, "Mutual information-based multi-auv path planning for scalar field sampling using multidimensional rt," *IEEE Transactions on Systems, Man, and Cybernetics: Systems*, vol. 46, no. 7, pp. 993–1004, 2015.
- [30] B. J. Julian, M. Angermann, M. Schwager, and D. Rus, "Distributed robotic sensor networks: An information-theoretic approach," *The International Journal of Robotics Research*, vol. 31, no. 10, pp. 1134–1154, 2012.
- [31] C. Rasmussen and C. Williams, *Gaussian Processes for Machine Learning*. MIT Press, 2006.
- [32] Y. Cao, Y. Wang, A. Vashisth, H. Fan, and G. A. Sartoretti, "Catnipp: Context-aware attention-based network for informative path planning," in *Conference on Robot Learning*. PMLR, 2023, pp. 1928–1937.
- [33] J. Schulman, F. Wolski, P. Dhariwal, A. Radford, and O. Klimov, "Proximal Policy Optimization Algorithms," *arXiv preprint arXiv:1707.06347*, 2017.
- [34] J. Ott, E. Balaban, and M. J. Kochenderfer, "Sequential bayesian optimization for adaptive informative path planning with multimodal sensing," in *Proc. of the IEEE Int. Conf. on Robotics and Automation (ICRA)*, 2023, 2023.
- [35] D. Peralta, J. Casimiro, A. M. Nilles, J. A. Aguilar, R. Atienza, and R. Cajote, "Next-best view policy for 3d reconstruction," in *Computer Vision—ECCV 2020 Workshops: Glasgow, UK, August 23–28, 2020, Proceedings, Part IV 16*. Springer, 2020, pp. 558–573.